Strojniški vestnik - Journal of Mechanical Engineering 56(2010)2, 104-114
UDC 621.785
Paper received: 19.11.2009
Paper accepted: 19.01.2010

Prediction of Quench-Hardness within the Whole Volume of Axially-Symmetric Workpieces of any Shape

Božidar Liščić[1] - Saša Singer[2] - Božo Smoljan[3]
[1] University of Zagreb, Faculty of Mechanical Engineering, Croatia
[2] University of Zagreb, Department of Mathematics, Croatia
[3] University of Rijeka, Faculty of Engineering, Croatia

A quench probe, based on temperature gradient method was used to measure and record cooling curves when quenching real axially symmetric workpieces of any complex shape in liquid quenchants. Calculation of relevant heat transfer coefficients (HTC) is based on the cooling curve measured just below surface of the cylindrical probe of 50 mm diameter. A 2-D computer program, based on the cooling time from 800 to 500°C ($t_{8/5}$), and the Jominy hardenability curve of the steel grade in question, is used to predict the hardness distribution within the whole volume of the workpiece, all at once, which is a unique feature of this method.

Keywords: quenching, heat transfer coefficient, hardness prediction

0 INTRODUCTION

For scientific investigation computer aided prediction of hardness distribution after quenching is usually done on perpendicular cross-section of a cylindrical specimen, presented as a hardness curve from the surface to the core. This information is valuable because it can show differences when different quenching conditions are used. However, it is valid only for the solid cylinder of specimen's diameter. Real workpieces in practice are seldom simple cylinders. Although being axially-symmetric they have different diameters, recesses and/or axial holes (Fig. 1).

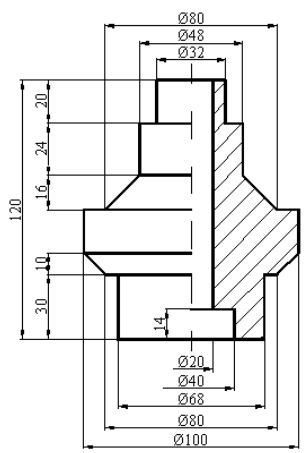

Fig. 1. *Example of a real axially-symmetric workpiece*

Each perpendicular cross-section in this case is different. This implies that on the axial section the thicknesses of material are different. They cool with different cooling rates at quenching, resulting in different hardness values in different points. For the workshop practitioners, the main interest is to see at once the hardness distribution in all points of the volume, so that they can evaluate the achieved depth of hardening. If they are not satisfied with it, they can repeat the simulation using other quenchant and/or quenching condition, or another steel grade. Such simulations are the main aim of the described method. The fundamental prerequisite for any successful simulation of a quenching process is the real description of the heat transfer, as input value for the calculation.

1 CALCULATION OF THE HEAT TRANSFER COEFFICIENT (HTC)

Any quenching process in evaporable liquids is a complex thermo-and fluiddynamic problem, described in chapter 3 of [1], encompassing different phases (vapour film, nucleate boiling and convection). To describe the heat transfer from a heated metallic workpiece to the quenchant, determination of the temperature dependent heat transfer coefficient (*HTC*) is used.

To calculate the *HTC*, a cooling curve measured near the surface of the probe is necessary. In this investigation, a cylindrical probe of 50 mm d × 200 mm, instrumented with 3

*Corr. Author's Address: Faculty of Mechanical Engineering, Ivana Lucica Street 5, 10000 Zagreb, Croatia, bliscic@fsb.hr

thermocouples (1 and 4.5 mm below surface and in the centre), situated all at the same radius, in the mid-length of the probe, is used. Fig. 2 shows the recorded cooling curves.

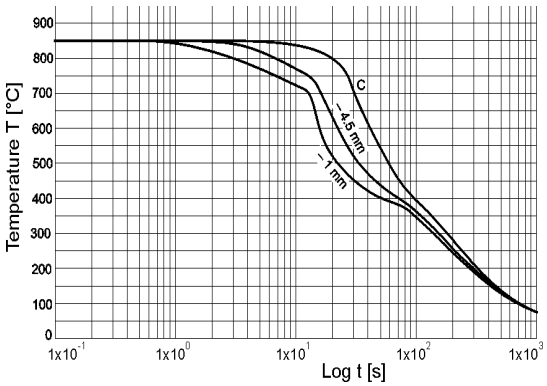

Fig. 2. *Experimentally obtained cooling curves (T-t) when quenching the 50 mm d × 200 mm probe instrumented with three thermocouples, in a high-speed mineral oil of 50 °C, without agitation [2]*

Due to the length to diameter ratio of 4:1 of the probe, the heat transferred through both ends is negligible, and the probe can be considered a long radially symmetric body of a given radius "*r*". In a simplified one-dimensional model, the temperature distribution $T(x,t)$ inside the cylinder, for times $t > 0$, depending only on the radial distance x [0, r] from the centre of the cylinder, is determined by the one-dimensional heat conduction equation:

$$\rho \cdot c \cdot \frac{\partial T}{\partial t} = \operatorname{div}\left(\lambda \operatorname{grad} T\right). \tag{1}$$

All physical properties: ρ (density); c (specific heat capacity) and λ (heat conductivity) of the probe's material are temperature dependent, so the whole problem is nonlinear. The initial condition $T(x, 0)$ is known (measured), and the problem is to determine the surface heat transfer coefficient "α" in the boundary condition for $x = r$:

$$\lambda \cdot \frac{\partial T}{\partial x} = -\alpha\left(T - T_{\text{ex}}\right) \tag{2}$$

where $T_{\text{ex}}(t)$ is the measured external temperature of the quenchant. To determine α, an additional cooling curve $T(t)$ is measured at a point $x = r_1$ near the surface (in this case 1 mm below surface). The inverse problem of computing α is solved by the following numerical procedure:

1. Solve the heat conduction Eq. (1) within the range $[0, r_1]$ with measured $T(t)$, as Dirichlet boundary condition.
2. If $r_1 < r$, extend the solution towards the boundary, from $[0, r_1]$ to $[0, r]$.
3. Calculate α from Eq. (2) with measured $T_{\text{ex}}(t)$, by using numerical differentiation.

- Since temperatures are measured at discrete times, they have to be smoothed before use. This is done by cubic spline least-squares approximation, to get sufficiently smooth global approximation over the whole time range.
- Numerical solution of the heat conduction Eq. (1) is done by the nonlinear implicit method, with simple iterations per time step, to adjust all physical properties to new temperatures.
- The solution extension in step 2 is computed by local extrapolation, based on low degree polynomial least squares approximation. The same approximation is also used for numerical differentiation needed to compute α in step 3.

How realistic and exact the determination of the *HTC* will be, depends also on the input data from the point where the temperature inside the probe is measured. These data can be influenced by the following phenomena:

a) Damping effect

In case of very fast changing temperatures on the surface of a body, the maximum values of this change will not be recorded, if temperature is measured below the surface. The greater the distance from the surface, the greater the damping effect, as shown in Fig. 3. Therefore, the position of the thermocouple should be as close as possible to the surface.

b) Time lag

It represents the time required for a sensor (in this case thermocouple) at a distance "*l*" below surface, to sense changes in surface condition, which are delayed because of thermal diffusivity. It can be calculated as follows:

$$a\,\delta t / l^2 = 0.06, \quad \delta t = 0.06\,\frac{l^2}{k/\rho c}. \tag{3}$$

where δt [s] is time lag, l [m] is distance from surface, a [W/m^{2}J] is thermal difusivity, k [W/(mK)] is thermal conductivity, c [J/(kgK)] is specific heat capacity, ρ [kg/m^3] is density .

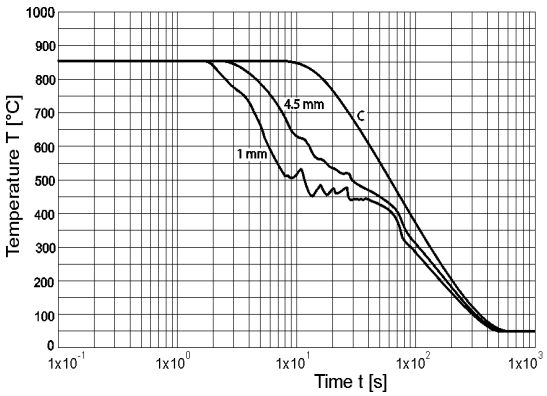

Fig. 3. *Damping effect when a probe of 50 mm Dia. was quenched in a polymer-solution of 35°C, with agitation [2]*

c) Thermocouple (TC) response time

During very fast temperature changes on the surface, the conventional sheathed TC below the surface may not follow the real time-temperature changes because of its slow response time. A TC of e.g. 3.175 mm outer diameter has two round wires of 0.5 mm diameter insulated from each other by about 0.38 mm of Al_2O_3, as shown in Fig. 4a. The Al_2O_3 is an insulator with very low thermal conductivity. Once it is heated up, it cools relatively slowly (it acts as a heat reservoir). As a result at any instant of time during the rapid cool-down phase, the Al_2O_3 is hotter than the thermal junction. It then tends to inhibit the cool-down of the junction, and hence this TC indicates a temperature which is higher than the real temperature (at that point without the sensor), at that instant of time. The time constant (63.2% of its total output signal, when subjected to a step-change in temperature) of the described TC is 3.5 seconds. In order to reach 99% of its full output, the time constant has to be multiplied by 5, which makes 17.5 seconds, as shown in Fig. 4b.

Therefore, any temperature change that occurs in less than 17.5 seconds will not be read accurately, but in such cases this TC will read a temperature which is both reduced in amplitude and delayed in time. It should be mentioned, however, that the time constant is determined by rapid immersion of the TC alone into hot oil bath, while in case of a quench probe the TC is embeded into the probe's body and cools down together with it. Therefore, it is questionable whether or not the above described time constant is fully applicable in this case. In any case to minimize the TC response time, according to Fig. 4b, the TC with the smallest possible outer diameter (*OD*) should be used for measuring fast changing temperatures.

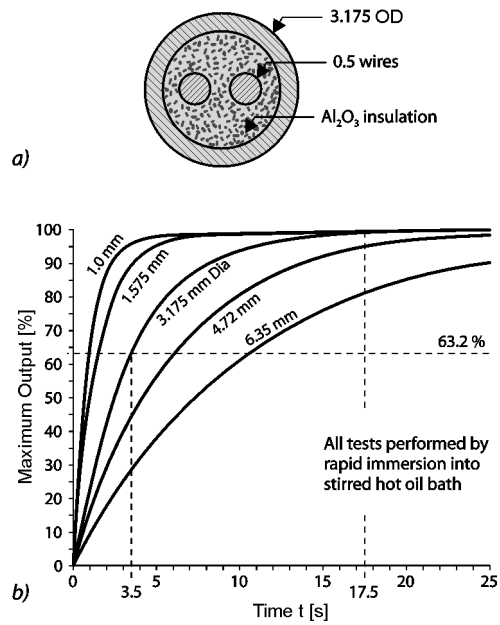

Fig. 4. *a) Cross-section of the 3.175 mm outer diameter stainless-steel sheathed thermocouple b)Response times of sheathed grounded thermocouples with different outer diameters [3]*

2 PECULIARITIES OF THE HEAT TRANSFER COEFFICIENT WHEN QUENCHING REAL WORKPIECES

2.1 Differences of the *HTC* over the Entire Surface of the Workpiece

Depending on the shape of the workpiece, big differences of *HTC* values are possible at different points over the entire surface, as shown in Fig. 5 for a relatively simple workpiece. Other factors that affect the *HTC*, besides the quenchant are: surface roughness, local flow field and its turbulence.

Therefore, a compromise has to be made when using a 1-D calculated *HTC* of a cylindrical probe, for a real workpiece of complex shape. In any case care should be taken that the basic shape of the probe (cylinder, plate, ring) corresponds to basic shape of the workpiece.

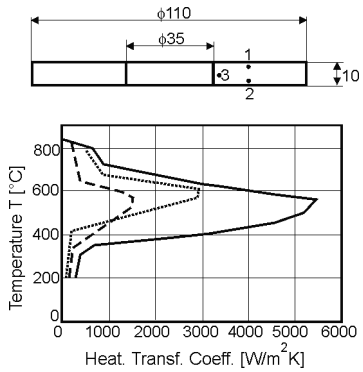

Fig. 5. *HTC at different points of a flat ring quenched horizontally in still oil of 70°C [4]*

2.2 Influence of the Probe Diameter on the Calculated HTC

Does the diameter of an axially symmetric workpiece, even a simple cylinder, have an influence on the *HTC* as function of surface temperature? Without answering this question, it is impossible to know in which span of diameters a calculated *HTC* may be used.

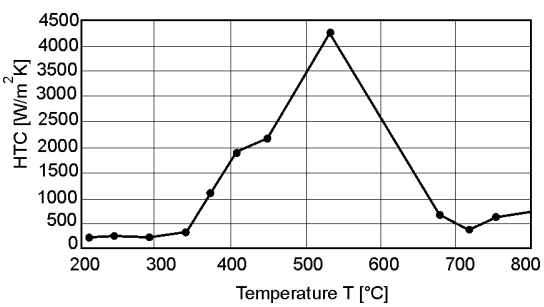

Fig. 6. *Calculated HTC of an ISO-9950 standard laboratory test probe (12.5 mm d × 60 mm) quenched in fast quenching oil [5]*

Fig. 6 shows a *HTC* vs. surface temperature of the standard cylindrical laboratory test probe quenched in a fast quenching oil with the maximum value of 4250 W/(m^{2}K). The calculation was based on an inverse heat conduction algorithm, which uses an iterative procedure that begins with an initial guess to calculate the temperature dependent *HTC* [5]. In this case the thermocouple which has recorded the time-temperature history was placed in the geometric centre of the probe. Fig. 7 shows the *HTC* vs. time and vs. surface temperature, when quenching the 50 mm d × 200 mm probe in a still mineral oil of 20°C. The maximum value of the calculated *HTC* is 1400 W/(m^{2}K). Calculation of the *HTC* was based on the control volume numerical method [7]. In this case the surface temperature of the probe was directly measured, using a special "self-renewing" thermocouple (U.S.Pat. No. 2,829.185). It is difficult to judge which of the following factors contributed more to the difference in *HTC*: the cylinder diameter, the calculation method, or the position of the thermocouple?

In order to investigate only the influence of the diameter on *HTC*, computer simulations have been performed for cylinders of 20 and 80 mm diameter, using the *HTC* for 50 mm diameter shown in Fig. 7. The same control volume method for calculation was used.

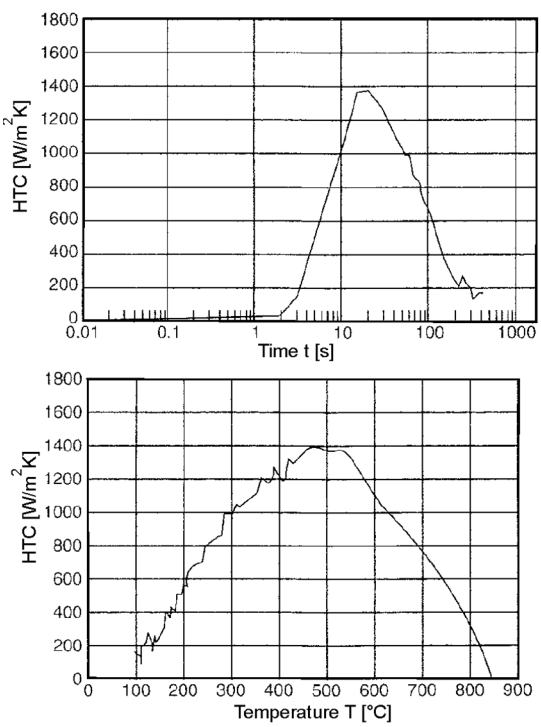

Fig. 7 *HTC a) vs. time and b) vs. surface temperature, when quenching the 50 mm Dia. × 200 mm probe in a still mineral oil of 20 °C [6]*

The results of these simulations showed no difference of *HTC* vs. temperature, compared to Fig. 7, but there were differences in *HTC* vs. time. As shown in Fig. 8 the time to achieve the

maximum value of the *HTC* is 10 seconds for 20 mm diameter, but 14 seconds for 80 mm diameter, as shown in Fig. 9. Also the area under the *HTC* curve in case of 80 mm diameter is much bigger than in case of 20 mm diameter.

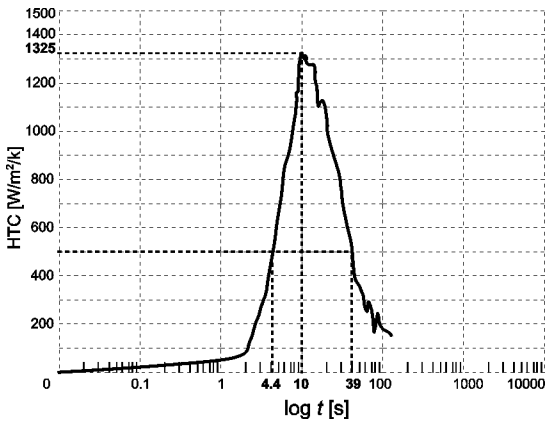

Fig. 8. *HTC vs. time for a cylinder of 20 mm d x 80 mm, quenched in still mineral oil of 20 °C, calculated by means of the heat transfer coefficient for cylinder of 50 mm d x 200 mm [7]*

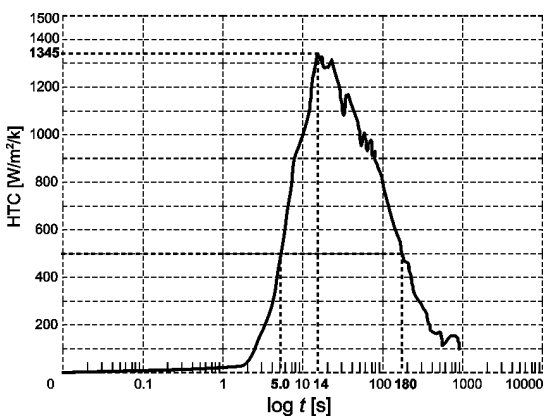

Fig. 9. *HTC vs. time for a cylinder of 80 mm d x 320 mm, quenched in still mineral oil of 20 °C, calculated by means of the heat transfer coefficient for cylinder of 50 mm d × 200 mm [7]*

According to the Nukiyama curve for boiling [1], as shown in Fig. 10, the *HTC* curve *(α)* follows the heat flux density curve *(q)*; accordingly the area under the *HTC* curves in Figs. 8 and 9 also represents the heat extracted. From these simulations the following can be concluded: if calculations for smaller or bigger diameters are performed with a known *HTC* of a certain cylinder diameter, the maximum value of *HTC* will not change, but to find the difference, the curves *HTC* vs. time should be compared. These differences are in accordance with the cooling curves for different cylinder diameters.

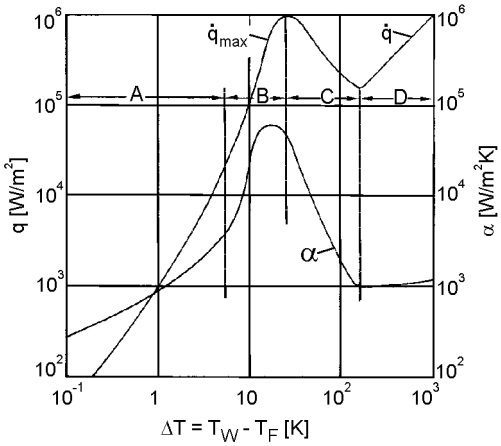

Fig. 10. *Nukiyama curve for boiling. A-free convection; B-nucleate boiling; C-transition boiling; D-film boiling [1]*

2.3 Influence of Wetting Kinematics on the *HTC*

Wetting kinematics is accompanied with every quenching process in evaporable liquids, and can influence more or less the *HTC*. As shown in Fig. 11 rewetting starts in those places on the workpiece surface where the film boiling (vapour blanket) collapses and nucleate boiling starts.

At every of these places at that moment a sudden increase of the *HTC* occurs. When cylinders with smooth surface are involved, rewetting starts usually at the lower end and moves gradually as a "wetting front" towards the upper end, as it is shown on the left side of Fig. 12. Temperature inside the cylinder changes not only radially, but also along the cylinder *(z)*, as it is shown on the right side of the same figure. The rewetting process on the cylinder surface causes axial heat fluxes. This process can have different forms and durations (from slowly moving wetting front at e.g. quenching oil of higher temperature, to abrupt explosion at some polymer solutions), so it can have smaller or bigger influence on the local *HTC*. This phenomenon is today an object of scientific research in laboratory conditions, but it is not yet taken into consideration when calculating *HTC* of real workpieces.

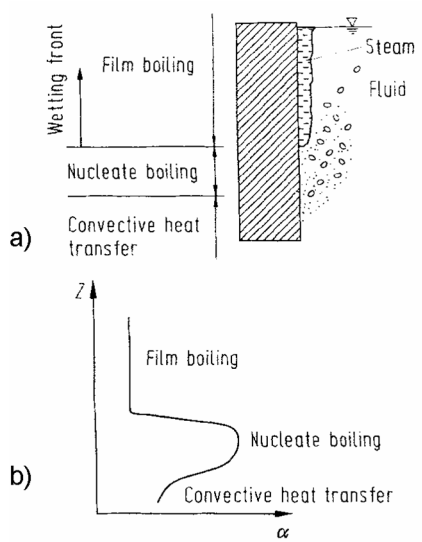

Fig. 11. *Change in HTC at immersion cooling due to wetting kinematics [8]*

3 PREDICTION OF HARDNESS DISTRIBUTION WITHIN THE WHOLE VOLUME OF THE WORKPIECE AFTER QUENCHING

To predict the hardness distribution, at once, within the whole volume of the quenched axially-symmetric workpieces of any shape, a 2-D computer program was developed [10] and [11].

The program is based on the Finite Volume Method and also contains the necessary subroutine for drawing a 2-D contour of every axially-symmetric workpiece, and automatic generation of the FE mesh for a symmetrical half of it. By using temperature dependent *HTC* calculated for each concrete case of quenching, cooling curves at every particular point of the axial workpiece section are calculated, and cooling times from 800 to 500°C ($t_{8/5}$) determined.

According to Rose [12] the time $t_{8/5}$ is a relevant characteristic for phase transformation in most structural steels Fig. 13. Accordingly it is a decisive feature for the resulting hardness after quenching. For every cooling curve in the CCT diagram shown (Fig. 13) the cooling time to 500 °C can be read on the time scale.

To determine the portions of structural phases and hardness after quenching, one should follow the relevant cooling curve until its intersection with the 500°C isotherm, and from this point down along the vertical line read the phase portions after quenching. For example, for the cooling curve C which intersects the 500°C isotherm at 135 seconds, the readings are: 4% ferrite, 7% pearlite, 78% bainite and 11% martensite. This combination of structural phases

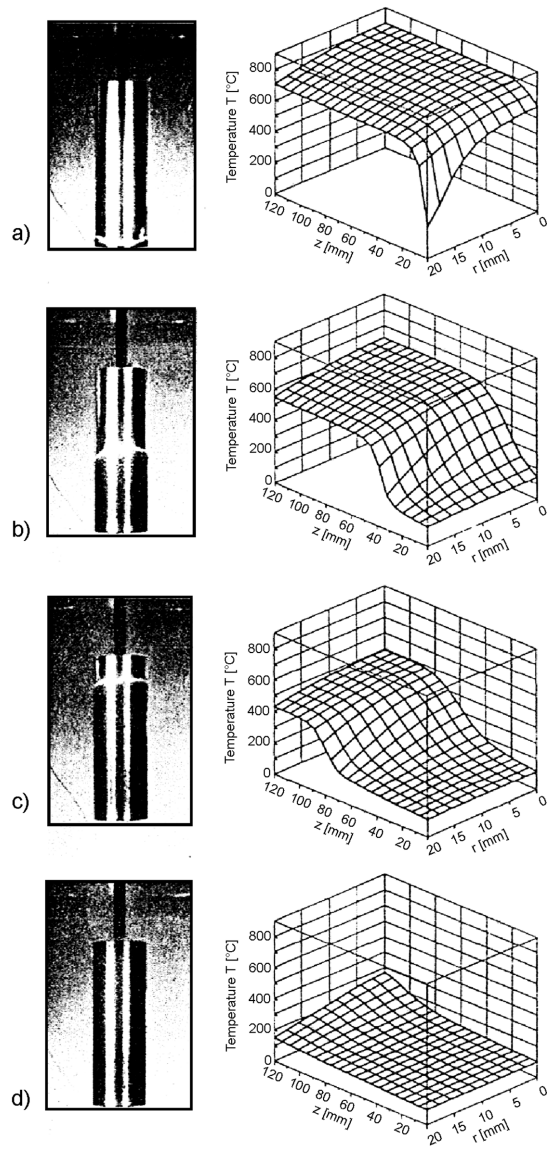

Fig. 12. *Observed wetting kinematics (left) and temperature distribution (right), calculated using local heat transfer coefficients, when immersion cooling AISI 4140 steel cylinders of 40 mm d × 120 mm in water of 80°C [9]*

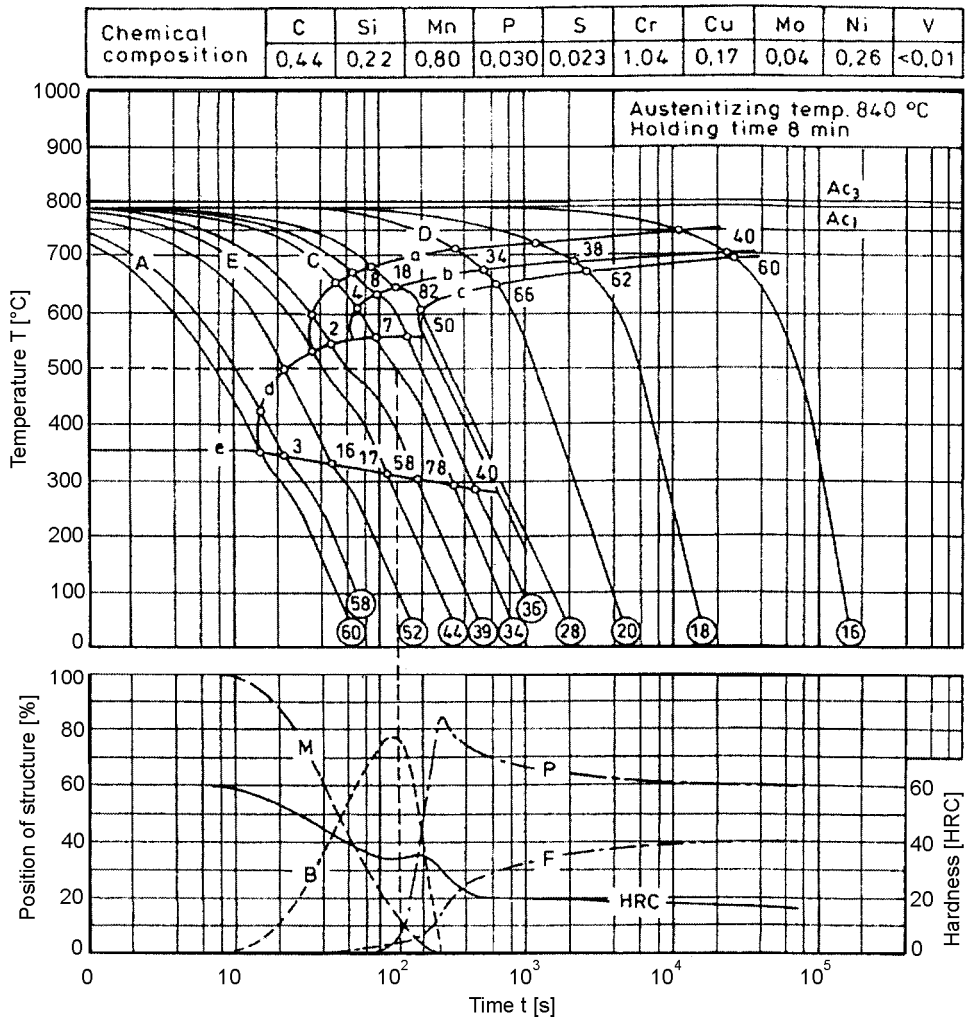

Fig. 13. *Continuous-Cooling-Transformation (CCT) diagram of the steel DIN 41Cr4 (top), with the diagram at bottom showing portions of each structural phase and hardness after quenching, depending on the cooling time to 500 °C*

for the steel in question (DIN 41Cr4) results with the quench-hardness of 34 HRC. Because there is a fixed relation between the cooling time $t_{8/5}$ and the distance from the quenched end of the Jominy specimen, as shown in Fig. 14, for each time $t_{8/5}$ the corresponding Jominy distance can be read. The next step is to read the hardness at the relevant Jominy distance from the Jominy hardenability curve of the concrete steel in question. The whole procedure of conversion the cooling time $t_{8/5}$ to the hardness at particular point of the workpiece section is shown schematically in Fig. 15.

The precision of the hardness prediction first depends on the Jominy curve, which further depends on the chemical composition of the particular batch, of every steel grade.

Therefore, the most precise hardness prediction can be expected when the Jominy curve for a particular batch of the relevant steel grade is available. Fig. 16 shows the results of hardness prediction across half of the axial section of a complex axially-symmetric workpiece made of steel DIN 41Cr4, a) without central hole, b) with central hole, quenched in oil.

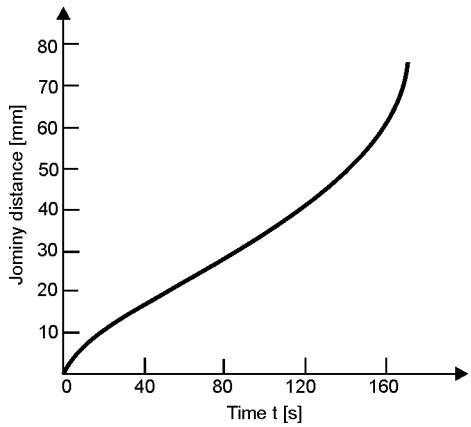

Fig. 14. *Relation between time of cooling from 800 to 500 °C ($t_{8/5}$), and the Jominy distance [12]*

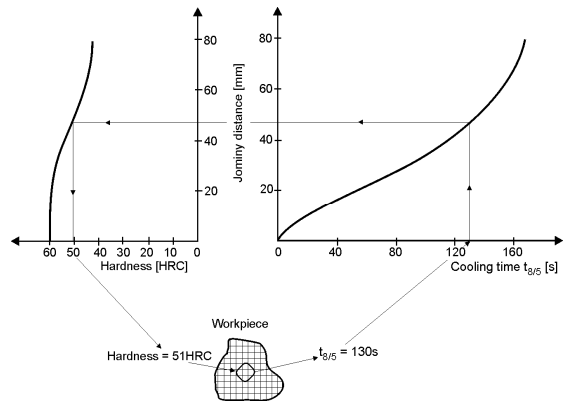

Fig. 15. *An example of conversion the cooling time $t_{8/5}$ to the hardness in a particular point of section*

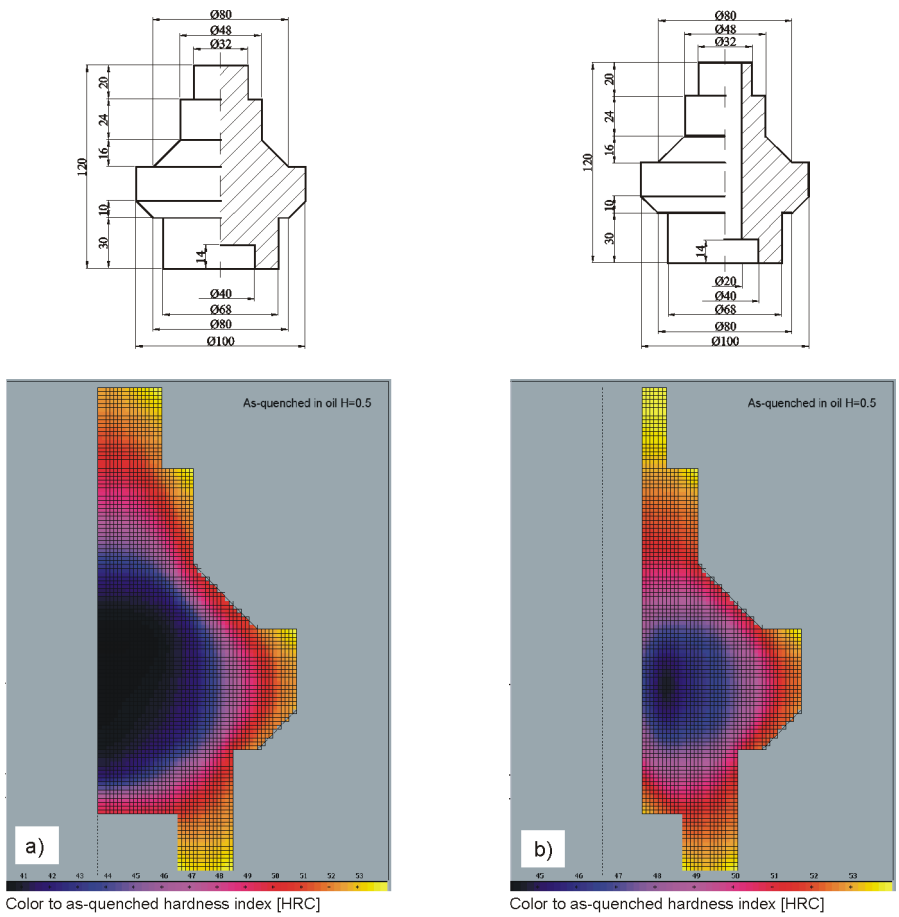

Fig. 16. *Results of hardness prediction across half of the axial section of a complex axially-symmetric workpiece made of steel DIN 41Cr4, quenched in oil; a) without central hole; b) with central hole of 20 mm diameter*

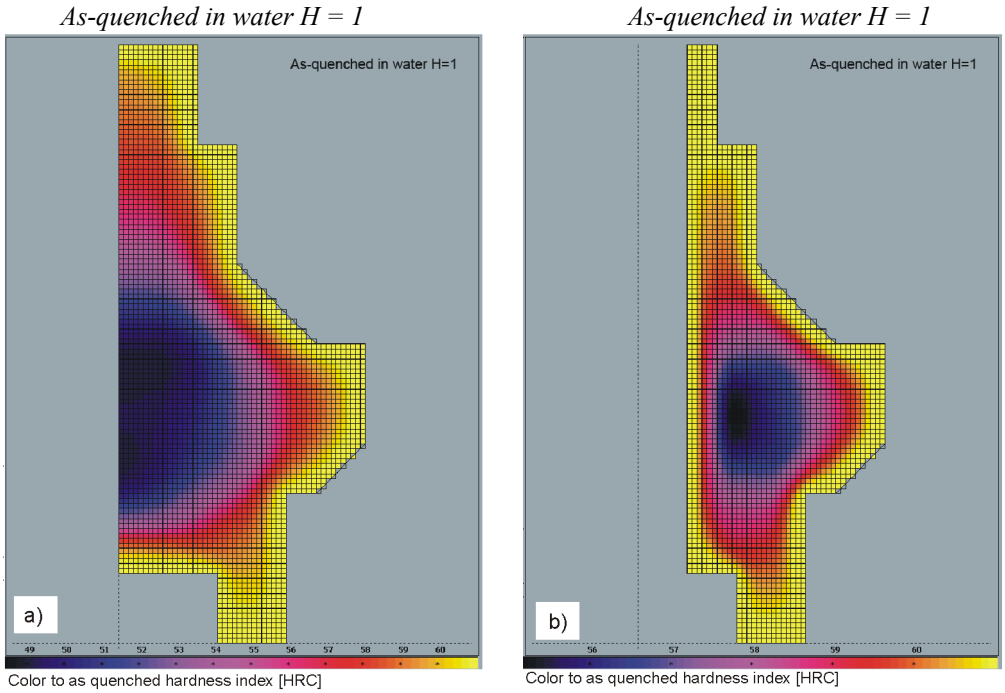

Fig. 17. *Results of hardness prediction for the workpiece shown in Fig. 16, made of the same steel DIN 41Cr4, quenched in still water*

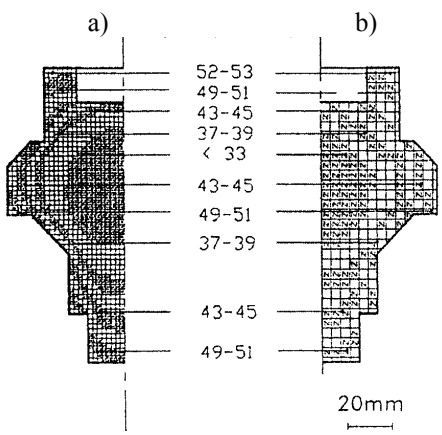

Fig. 18. *Hardness distribution across the section of the workpiece shown in Fig. 16, after quenching in oil: a) by mathematical modelling; b) by experiment [13]*

This case clearly shows that the applied Finite Volume Method effectively simulates cooling not only at the outer radii along the workpiece, but also at the inner radii in the hole. The hardness values in every particular point of the cross-section are determined by means of the color scale and relevant numbers depicted in HRC. As the same color nuance does not always also mean the same hardness, the color nuance should be always compared with associated numbers above the color scale.

The possibility to see the hardness values at once in all points of the axial section of a workpiece, and instantly conclude about the depth of hardening, is a special feature of this software. Fig. 17 shows the results of hardness prediction for the same workpiece shown in Fig. 16, made of the same steel, after quenching in water ($H = 1.0$). Fig. 18 shows the comparison between the predicted and experimentally obtained hardness distribution across the section of the workpiece shown in Fig. 16. The statistical survey for this workpiece has shown that differences between the predicted and measured hardness values have a standard deviation of 1.6 *HRC*.

4 PREDICTION OF HARDNESS AND MECHANICAL PROPERTIES AFTER QUENCHING AND TEMPERING

In some cases, particularly when dealing with steels for hardening and tempering, the hardness distribution after quenching and after tempering is of interest. There is a known relation

Quenched in oil H = 0.5 and tempered at 560°C

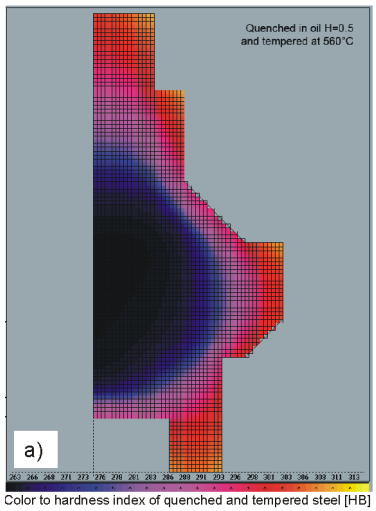

Quenched in oil H = 0.5 and tempered at 560°C

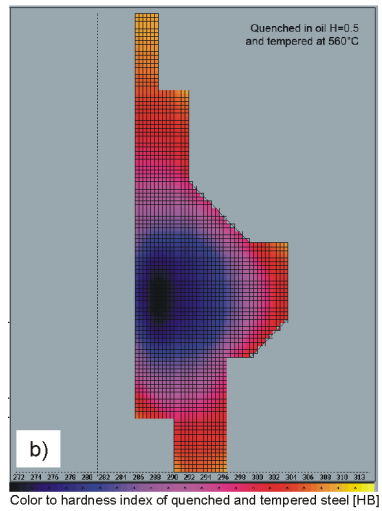

Fig. 19. *Results of hardness prediction for the workpiece shown in Fig. 16, made of the same steel DIN 41Cr4, quenched in oil and tempered at 560 °C*

between the hardness after quenching and the hardness after tempering:

$$HRC_{\text{tempered}} = \frac{HRC_{\text{quenched}}}{K} \tag{4}$$

$$K = C_1 \cdot t^{n_1} \cdot \exp\left[A\left(\frac{a}{T_{\text{temp}}} \right)^{n_2} - B \right] \tag{5}$$

where $T_{\text{temp.}}$ [K] is tempering temperature, t [h]is tempering time, A, B, C_1, a, n_1, n_2 are material constants.

Fig. 19 shows the results of hardness prediction for previously shown workpieces after quenching in oil and tempering at 560°C. The hardness scale is given in Brinell units.

By using an auxiliary diagram shown in Fig. 20 (the abscissa of which is compatible with the diagram of hardness distribution after tempering), a rough estimation of most common mechanical properties: Ultimate tensile strength [MPa], Yield strength [MPa], Elongation [%], is possible.

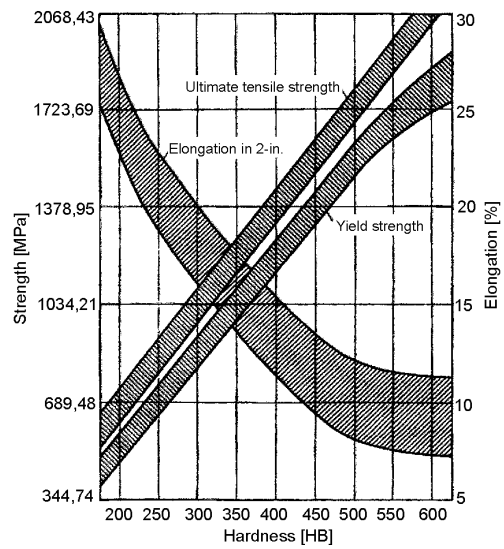

Fig. 20. *Range of tensile properties in several quenched and tempered steels at the relevant hardness values [14]*

5 CONCLUSION

In order to predict the hardness distribution within the whole volume of axially-symmetric workpieces, quenched in liquid quenchants, a 2-D computer program has been developed, based on the cooling time from 800 to 500 °C, and the Jominy hardenability curve of the relevant steel. The most important input for the necessary calculation is the *HTC*. The calculation of temperature dependent *HTC*, when real workpieces are involved, is based on cooling curve obtained by measuring and recording the time-temperature history at a point near the

surface of a special probe. Peculiarities of the *HTC*, when quenching real workpieces, as well as phenomena which can influence the accuracy of calculated *HTC*, have been discussed. When structural steels for hardening and tempering are used, the possibility to predict the hardness distribution, as well as some common mechanical properties after quenching and tempering, has been shown.

6 REFERENCES

[1] Liščić, B., Tensi, H.M., Luty, W. (1992) *Theory and Technology of Quenching*, Springer-Verlag, p. 41-72.

[2] By courtesy of PETROFER H.R. Fischer GmbH & Co KG, Römerring 12-16, D-31137 Hildesheim, Germany.

[3] Nanigian, J. (1994) Improving accuracy and response of thermocouples in ovens and furnaces, *Proceedings of Intl. Heat Treating Conference Equipment and Processes*, Schaumburg, p. 171-174.

[4] Segerberg, S., Bodin, J. (1992) Variation in the heat transfer coefficient around components of different shapes during quenching, *Proceedings First Intl. Conference on Quenching & Control of Distortion,* Chicago.

[5] Troell, E., Kristoffersen, H., Bodin, J., Segerberg, S., Felde, I. (2007) Unique software bridges the gap between cooling curves and the result of hardening, *HTM*, vol. 62, no. 3, p. 110-115.

[6] *Steel Heat Treatment* – Second Edition (2007) *Metallurgy and Technologies*, Totten, G.E. (Ed), Taylor & Francis Group, Boca Raton, p. 382.

[7] Proprietary program: *Simulation of Cooling a Cylinder in the Surrounding of Arbitrary Chosen Temperature*, Faculty of Mech. Engineering, University of Zagreb, Zagreb.

[8] Tensi, H.M. (1992) Wetting Kinematics (Chapter 5) in : *Theory and Technology of Quenching*, Springer-Verlag, p. 95.

[9] Majorek, A., Müller, H., Macherauch, E. Computer simulation of cooling steel cylinders by immersing in evaporable liquids, *HTM*, vol. 51, no. 1, p. 11-18.

[10] Smoljan, B. (1998) Numerical simulation of as- quenched hardness in a steel specimen of complex form, *Communications in Numerical Methods in Engineering*, vol. 14, p. 277-285.

[11] Smoljan, B (2002) Numerical simulation of steel quenching, *Journal of Materials Engineering and Performance*, vol. 111, no. 1, p. 75-80.

[12] Rose, A. et.al. (1958) *Atlas for heat treatment of steels I*, Verlag Stahleisen, Düsseldorf.

[13] Smoljan, B. (2000) Mathematical modelling of residual stress distribution in a quenched steel specimen, *Proceedings of the 12th IFHTSE Congress*, Melbourne, vol. 2, p. 217-222.

[14] *ASM Handbook*, (2000), Material Park, OH, ASM International, vol. 8, p. 27.